Self-Assembled Growth of ZnS Nanobelt Networks

Ping'an Hu, Yunqi Liu,* Lei Fu, Lingchao Cao, and Daoben Zhu*

Center for Molecular Science, Institute of Chemistry, Chinese Academy of Sciences, Beijing 100080, P. R. China

Received: September 15, 2003

By using a H_2-assisted thermal evaporation approach, ZnS nanobelts were grown on a Si substrate and self-assembled into a network structure. A vapor-solid process coupled with vapor−liquid−solid process is proposed for the formation of the ZnS nanobelts and their assembly. This functional structure may be well applied in the study of the electronic properties of ZnS nanobelts and other devices.

Introduction

One-dimensional (1D) nanoscale materials such as carbon nanotubes (CNTs)[1] and semiconductor nanowires[2] exhibit interesting and useful properties and may be applied as building blocks for the integration of the next generation of nanoelectronics and optics. A prerequisite for such integration is able to assemble the 1D nanomaterials in desired and functional structures. These involve generally two possible approaches: an in situ growth method and a post-growth fabrication method. As for the former, 1D nanomaterials grow parallel to the substrate, which is particularly important for their application in nanoscale electronics. The start and end of growth of 1D nanomaterials as well as their precise assembly into desired configuration on the substrate are usually determined by the pattern catalyst. Various lithographic techniques such as electronic beam, soft lithography, and photolithography are used to fabricate the pattern catalyst. For example, Dai et al. have demonstrated the SWNTs suspend bridge structure grown from the pattern catalyst.[3,4] It was reported that ZnO nanowires bridge the neighboring Au film pattern catalyst, and they formed an intricate network structure.[5] For the latter, the post-growth 1D nanomaterials assemble together and form a functional structure by suitable hierarchical assembly techniques. Atomic force microscopy (AFM) has been used to push or deposit SWNTs into a desired configurement,[6,7] but this method suffers from time-consuming work; the post-growth SWNTs aligning with electric field in liquids have been demonstrated, but this method has not been successful thus far due to poor SWNTs solubility in liquids.[8] Recently, microfluid-assisted assembly techniques have been reported to assemble 1D semiconductor nanowires between the microscale metal electrodes and fabricate semiconductor nanowire-based logic gates and computation devices as well as other electronic nanodevices.[9−11] Most of the reported approach used above for integration of 1D nanomaterials involves various lithographic techniques such as electronic beam, soft lithography and photolithography. Here we report in situ assembly of ZnS nanobelts during the growth process without the assistance of any lithographic technique.

ZnS, as an important group II−group IV semiconductor compound with a wide band gap energy of 3.7 eV, has attracted much research interest due to its excellent properties of luminescence and photochemistry. ZnS is a versatile and excellent phosphor host material and shows a variety of luminescence properties such as photolumeninescent,[12] cathodoluminescent,[13] electroluminescent[14] and thermoluminescent properties,[15] which enable it to have applications in the fields of flat displays, sensors, and lasers. In addition, ZnS behaves an effective catalyst and has attracted the attention in the fields of photosynthesis and pollutant treatment.[16−18] The excited electrons on nc-ZnS and nc-CdS exhibit highly negative reduction potentials and the nanocrystallites are effective photocatalysts for the photoreduction of CO_2, aromatic ketones, amides, and electron-deficient alkenes under UV or visible light irradiation.[18] Recently, research interest in 1D ZnS nanomaterials is increasing because of their potential application in nanoscale electronics, optics and other novel devices. Nanowires, nanorods, and nanobelts of ZnS have been obtained by liquid-crystal template,[19] irradiation,[20] and solvothermal[21] and physical evaporation.[22−24] But no papers have yet been reported on the in situ assembly of 1D ZnS nanomaterial during their growth process.

Experimental Methods

In this paper, we provide a simple self-assembly approach without involving lithography to produce an in situ ZnS nanobelt network. Some of the ZnS nanobelt bridged two dots, which is very useful for the development of electrical nanoconnections and other devices. The ZnS nanobelt networks grew on a Si substrate in a quartz tube furnace using ZnS powder as the precursor and high pure Ar mixed with 3−8% H_2 as carrier gas at 900−1100 °C. The morphologies and chemical compositions of the products are characterized by a scanning electron microscope (SEM, JSM-6700F) equipped with an Oxford energy-dispersive X-ray detector (EDX, INCA300), a transmission electron microscope (TEM, Hitachi-800, JEOL-2010 F), and an X-ray diffraction instrument (XRD, Rigaku Dmax2000, Cu Kα).

Results and Discussion

Structure and Morphology of the ZnS Nanobelts Network. Figure 1a shows a typical structure of ZnS nanobelt networks synthesized at 950 °C. The nanobelts nucleated from one dot, and some nanobelts have one end resting between dots whereas some nanobelts bridge two dots to form the network structure. Figure 1b, which is a closer SEM image of the nucleate location,

* Corresponding authors. Telephone: +86-10-62613253. Fax: 86-10-62559373. E-mail (Y.L.): liuyq@iccas.ac.cn.

10.1021/jp036743z CCC: $27.50
Published on Web 12/24/2003

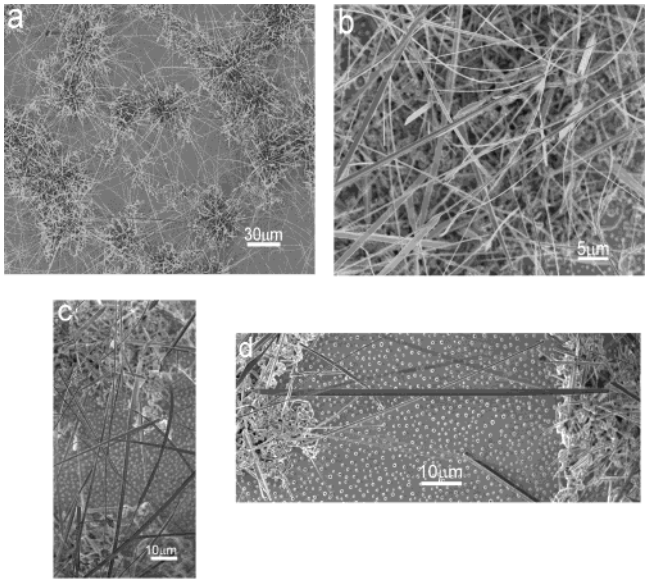

Figure 1. SEM images. (a) A typical network structure of ZnS nanobelts formed by self-assembly at 950 °C is shown. (b) The products mainly consists of ZnS nanobelts with widths of 0.5−5 μm that are tens to several hundred micrometers in length. (c) Several ZnS nanobelts sprouted from the nucleation and connected to the other, some wirelike materials are also observed. (d) A single ZnS nanobelt with a growth direction parallel to the substrate linked two nucleation sites.

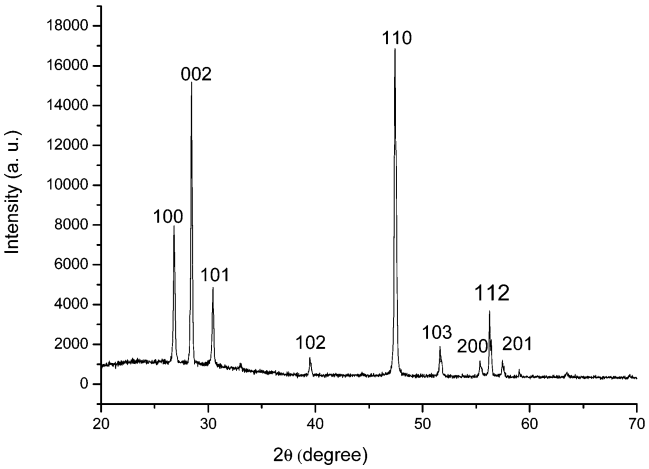

Figure 2. Typical X-ray diffraction pattern of the as-prepared products, showing a wurtzite structure.

shows that the products mainly consist of beltlike structures with an average width of 0.5−5 μm that are tens to several hundred micrometers in length. As shown in Figure 1c, which is a high magnification SEM image, several ZnS nanobelts sprouted from the nucleation and connected to the other, and some wirelike materials are also observed; the nanomaterials have disorder growth directions. As shown in Figure 1d, a single ZnS nanobelt with a width of 1.6 μm and a growth direction parallel to the substrate links two nucleation sites; a large quantity of ZnS nanocrystallines dispersed on the substrate and grew simultaneously with the ZnS nanobelts. From the energy-dispersive X-ray detector (EDX) analysis, these products are composed of Zn and S with an atomic ratio of about 1:1 within the limit of experimental error.

The products were structurally characterized by XRD. A typical XRD pattern is shown in Figure 2 with all diffraction peaks indexed to the known wurtzite structure phase of ZnS (JCPDS card No. 36-1450).

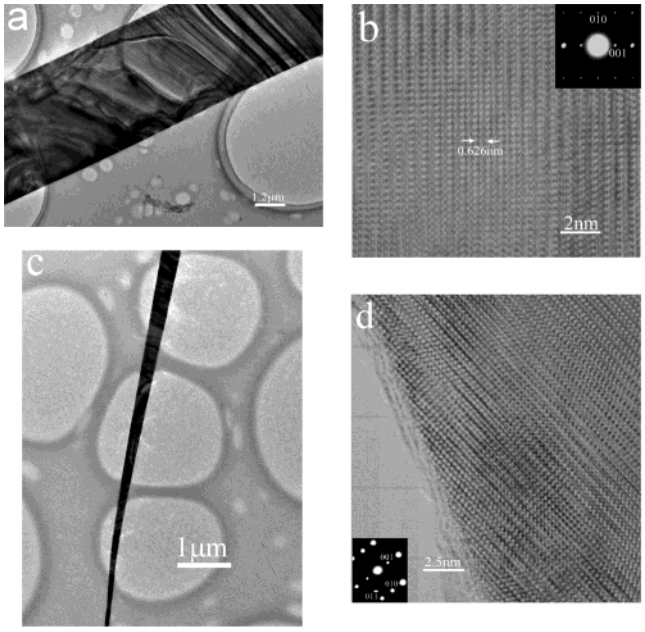

Figure 3. (a) Individual ZnS nanobelt with uniform width. (b) High-resolution TEM image with a SAED pattern revealing that ZnS nanobelt is highly crystalline and has a preferred growth direction; (c) ZnS nanobelt with a variational width. (d) High-resolution TEM image with a SAED pattern showing that the ZnS nanobelt has a diverse crystalline structure from above and a slight slip dislocation defect.

The structure and morphology of the ZnS nanobelts are further characterized by transmission electron microscopy. Most of the nanobelts have a uniform width and thickness along their entire length, typical widths and thickness are in the ranges 0.5−5 μm and 10−40 nm (Figure 3a). The ripplelike line in the TEM image is due to the bending of the nanobelts. A high-resolution TEM (HRTEM) given in Figure 3b shows a perfect wurtzite structure with a [100] zone axis, and the corresponding selected-area electron diffraction (SAED) is provided in the inset. The measured spacing of the crystallographic planes is 0.626 nm, which corresponds to the {001} lattice plane of hexagonal ZnS. In addition, as shown in Figure 3c a small quantity of nanobelts have a variety width along its length, while the thickness does not change. The HRTEM shown in Figure 3d with a corresponding SAED as an inset reveals a diverse crystalline structure from above and a slight slip dislocation defect.

The network may grow via a vapor−solid (VS) mechanism[25] combined with a vapor−liquid−solid (VLS) mechanism.[26] At first, ZnS are reduced into Zn gas and H_2S by H_2 at high temperature. At a lower temperature, some of the Zn gas formed into liquid drops of Zn, which partially dispersed on the substrate. The hot Zn ball on the wafer might dissolve the Si to form the Si−Zn alloys. The Si−Zn alloy ball absorbed the H_2S gas around it and ZnS nanobelts began to nucleate, and this process was governed by the VLS mechanism. At the same time, ZnS gas, which was quickly formed by Zn gas reacting with H_2S, flew to the low temperature area. At low temperature, due to the high supersaturation of ZnS, the ZnS gas directly deposited on the nucleation in a solid mode to grow ZnS nanocrystallines in a beltlike structure, while ZnS gas deposited on the bare substrate, where there was no nucleation, and formed nanoparticles. This process was controlled by a VS mechanism. Therefore, the growth of ZnS nanobelts involved both a VLS mechanism and a VS mechanism. We do not know the reason some of the ZnS nanobelt by themselves connected to the neighboring dots of nucleation to form a network structure.

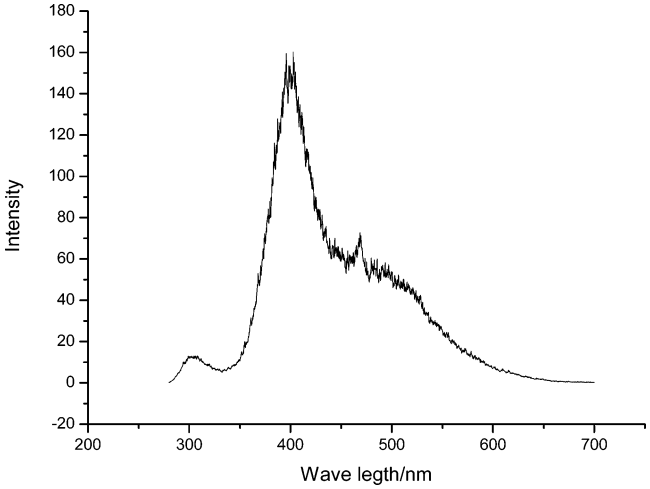

Figure 4. Photoluminescence spectra of the ZnS nanobelts.

Therefore, the detailed growth mechanism of ZnS belt network is not clear yet and should be further studied.

Optical Characterization of the ZnS Nanobelts. Room-temperature photoluminescence (PL) spectra of the ZnS nanobelts was measured by an F-4500 fluorescence spectrophotometer using a xenon discharge lamp as the excitation source. The excited wavelength is 250 nm, and the PL spectra shown in Figure 4 reveals a broad emission band centered at 401 nm and a weak shoulder peak at 470 nm. The first one at 401 nm may be attributed to a sulfur vacancy and interstitial sulfur lattice defects, which is reported in the literature.[27] A modest blue shift (∼40 nm) of the emission band position relative to that of the bulk ZnS (440−500 nm) might be due to the quantum size effects of the ZnS nanocrystals. The other at 470 nm is the well-known ZnS related luminescence of zinc vacancies (at ∼480 nm).[28]

Conclusion

In conclusion, by a H_2-assisted thermal evaporation approach, ZnS nanobelt networks were obtained on the Si wafer during in situ growth. This functional structure formed by 1D nanomaterial assembly may be well applied in the research of the electronic properties of ZnS nanobelts and in nanoscale devices.

Acknowledgment. The authors gratefully acknowledge financial support from the National Natural Science Foundation of China (NNSFC), the Major State Basic Research Development Program, and the Chinese Academy of Sciences

References and Notes

(1) Iijima, S. *Nature* **1991**, *354*, 56.
(2) Xia, Y.; Yang, P. *Adv. Mater.* **2003**, *15*, 351.
(3) Franklin, N. R.; Dai, H. *Adv. Mater.* **2000**, *12*, 890.
(4) Zhang, Y.; Chang, A.; Cao, J.; Wang, Q.; Kim, W.; Li, Y.; Morris, N.; Yenilmez, E.; Kong, J.; Dai, H. *Appl. Phys. Lett.* **2001**, *79*, 3155.
(5) Huang, M. H.; Wu, Y.; Feick, H.; Tran, N.; Weber, E.; Yang, P. *Adv. Mater.* **2001**, *13*, 113.
(6) Cheung, C. L.; Hafner, J. H.; Odom, T. W.; Kim, K.; Lieber, C. M. *Appl. Phys. Lett.* **2001**, *79*, 3136.
(7) Lefebvre, J.; Lynch, J. F.; Llaguno, M.; Radosavljevic, M.; Johnson, A. T.; *Appl. Phys. Lett.* **1999**, *75*, 3014.
(8) Chen, X. Q.; Saito, T.; Yamada, H.; Matsushige, K. *Appl. Phys. Lett.* **2001**, *78*, 3714.
(9) Huang, Y.; Duan, X.; Wei, Q.; Lieber, C. M.*Science* **2001**, *291*, 630.
(10) Huang, Y.; Duan, X.; Cui, Y.; Lauhon, L. J.; Kim, K.; Lieber, C. M. *Science* **2001**, *294*, 1313.
(11) Cui, Y.; Wei, Qi.; Park, H.; Lieber, C. M. *Science* **2001**, *293*, 1289.
(12) Falcony, C.; Garcia, M.; Ortiz, A.; Alonso, J. C. *J. Appl. Phys.* **1992**, *72*, 1525.
(13) Bredol, M.; Merikhi, J. *J. Mater. Sci.* **1998**, *33*, 471.
(14) Leeb, J.; Gebhardt, V.; Mu1ller, G..; Haarer, D.; Su, D.; Giersig, M.; McMahon,| G..; Spanhel, L. *J. Phys. Chem. B* **1999**, *103*, 7839.
(15) Chen, W.; Wang, Z.; Lin, Z.; Lin, L. *Appl. Phys. Lett.* **1997**, *70*, 1465.
(16) Yanagida, S.; Kawakami, H.; Midori, Y.; Kizumoto, H.; Pac, C. J.; Wada, Y. *Bull. Chem. Soc. Jpn.* **1995**, *68*, 1811.
(17) Fujiwara, H.; Hosokawa, H.; Murakoshi, K.; Wada, Y.; Yanagida, S. *Langmuir* **1998**, *14*, 5154.
(18) Yin, H.; Wada, Y.; Kitamura, T.; Anagida, S. Y. *Environ. Sci. Technol.*. **2001**, *35*, 227.
(19) Zhang, D.; Qi, L.; Cheng, H.; Ma, J. *J. Colloid Interface Sci.* **2002**, *246*, 413.
(20) Jiang, X.; Xie, Y.; Lu, J.; Zhu, L.; He, W.; Qian, Y. *Chem. Mater.* **2001**, *13*, 1213.
(21) Li, Y.; Liao, H.; Ding, Y.; Fan, Y.; Zhang, Y.; Qian, Y. *Inorg. Chem.* **1999**, *38*, 1382.
(22) Jiang, Y.; Meng, X.; Liu, J.; Xie, Z. Y. C.; Lee, S.; Lee, S. T. *Adv. Mater.* **2003**, *15*, 323.
(23) Zhu, Y.; Bando, Y.; Uemura, Y. *Chem. Commun.* **2003**, *7*, 836.
(24) Zhu, Y.; Bando, Y.; Xue,D. *Appl. Phys. Lett.* **2003**, *82*, 1769.
(25) Yang, P.; Lieber, C. M. *J. Mater. Res.*, **1997**, *12*, 2981.
(26) Morales, A. M.; Leiber, C. M. *Science* **1998**, *279*, 208.
(27) Becher, W. G.; Bard, A. G. *J. Phys. Chem.* **1983**, *87*, 4888.
(28) Zhang, W.-H.; Shi, J.-L.; Chen, H.-R.; Hua, Z.-L.; Yan, D.-S.*Chem. Mater.* **2001**, *13*, 648.